International Journal of Critical Infrastructures

ISSN online: 1741-8038 - ISSN print: 1475-3219
https://www.inderscience.com/ijcis

An edge computing-based fast restoration for urban medium- and low-voltage distribution networks

Zhaoyu Wu, Weirui Cai, Genyuan Zhang, Weichen Long, Lizhong Peng

DOI: 10.1504/IJCIS.2026.10076930

Article History:

Received:	13 November 2025
Last revised:	09 January 2026
Accepted:	10 January 2026
Published online:	16 March 2026

An edge computing-based fast restoration for urban medium- and low-voltage distribution networks

Zhaoyu Wu*, Weirui Cai, Genyuan Zhang and Weichen Long

Guangzhou Power Supply Bureau of Guangdong Power Grid Co., Ltd.,
Guang'zhou, 510630, China
Email: zywu@mls.sinanet.com
Email: cwrry1995@163.com
Email: 404779272@qq.com
Email: ycxlwc@126.com
*Corresponding author

Lizhong Peng

Dongfang Electronics Corporation,
Yantai, 264000, China
Email: 1099836072@qq.com

Abstract: The rapid and reliable restoration of urban medium- and low-voltage distribution networks is paramount for sustaining economic activities and social well-being. However, conventional centralised restoration methods are increasingly inadequate due to their inherent limitations in handling communication delays, heterogeneous real-time data integration, and the high computational complexity of stochastic optimisation, leading to prolonged outages and reduced service reliability. To address these challenges, this research proposes a fast power recovery method based on distributed edge computing for urban medium- and low-voltage distribution networks. The method enhances restoration efficiency through localised data processing, improved temporal performance, and the integration of heterogeneous data sources. Employing Box-Cox-combined Z-scale conversion for non-Gaussian temporal datasets and principal component-enhanced Dempster-Shafer deduction for information amalgamation, the approach transmutes multi-criteria recovery into singular-goal optimisation via decision matrices. Probabilistic voltage restrictions are reformulated as definitive quadratic mixed-integer constraints through sample average approximation, while second-degree conical relaxation manages non-linear current equations to establish a tractable mixed-integer quadratically constrained programming framework. Experimental outcomes demonstrate 2.89-minute recovery intervals, success probabilities exceeding 95%, and 0.82–0.91 load distribution equilibrium, exhibiting superior performance relative to comparative methodologies.

Keywords: edge computing; medium and low voltage distribution network; rapid restoration of power supply; DS reasoning mechanism.

Reference to this paper should be made as follows: Wu, Z., Cai, W., Zhang, G., Long, W. and Peng, L. (2026) 'An edge computing-based fast restoration for urban medium- and low-voltage distribution networks', *Int. J. Critical Infrastructures*, Vol. 22, No. 9, pp.1–21.

Biographical notes: Zhaoyu Wu received his Master's in Electrical Engineering from School of South China University of Technology. He is currently an Engineer in the Guangzhou Power Supply Bureau of Guangdong Power Grid Co., Ltd. He research interests include distribution network operation and power system analysis.

Weirui Cai received his Master's in Electrical Engineering from School of North China Electric Power University. He is currently an Engineer in the Guangzhou Power Supply Bureau of Guangdong Power Grid Co., Ltd. He research interests include distribution network operation and power system analysis.

Genyuan Zhang received his Bachelor's in Electrical Engineering from School of Northeast Electric Power University. He is currently an Engineer in the Guangzhou Power Supply Bureau of Guangdong Power Grid Co., Ltd. He research interests include distribution network operation, and artificial intelligence analysis.

Weichen Long received his Bachelor's in Electrical Engineering from School of North China Electric Power University. He is currently an Engineer in the Guangzhou Power Supply Bureau of Guangdong Power Grid Co., Ltd. He research interests include distribution network operation, new energy generation and power system analysis.

Lizhong Peng received his Bachelor's in Software Engineering from the School of Software Engineering, Hunan University in 2013. He is currently a mid-level Engineer at Dongfang Electronics Corporation, where he is primarily engaged in the research, development, and management of power systems and related projects. His research focuses on power system automation, computer applications, and software development.

1 Introduction

As urban expansion progresses and electricity demand intensity rises steadily, medium and low-voltage distribution grids – serving as the final segment of the electrical infrastructure – face direct impacts on urban economic operations and residential living standards due to their power reliability and swift recovery capabilities (Mannan et al., 2024; Kottmann et al., 2023; Zhang, 2022). These networks exhibit intricate topologies and extensive service ranges, rendering them susceptible to disruptions from environmental hazards, equipment deterioration, and operational errors, resulting in recurrent service interruptions (Yang et al., 2023). Contemporary electrical grids require faster restoration responses. However, conventional recovery methods lack flexibility in handling multifaceted failure scenarios, failing to meet metropolitan demands for ultra-reliable power supply (Yurov, 2022). These conventional approaches are fundamentally constrained by three intertwined challenges:

1 the latency and bandwidth limitations of transmitting massive, heterogeneous real-time data (e.g., from sensors, DERs, loads) to a central controller

2 the difficulty in fusing this multi-source data with conflicting or uncertain information to form a reliable system state awareness quickly

3 the computational intractability of solving large-scale, stochastic restoration optimisation models within the tight time window required for fast recovery.

Advanced fault detection and isolation systems, automated self-recovery control strategies, and the incorporation of decentralised generation offer innovative pathways for grid recuperation. Refining network reconfiguration methodologies and accelerating automated device reactions can drastically reduce interruption durations. Additionally, the adoption of advanced power electronics and digital communication systems enables the realisation of prompt and accurate power reinstatement (Kayal and Basumatary, 2023).

Consequently, investigating high-performance and adaptive rapid restoration approaches for medium- and low-voltage distribution systems holds substantial practical value for enhancing urban grid robustness and electricity delivery standards. Hu et al. (2023) introduced a grid recovery technique leveraging vehicle-to-grid (V2G) integration, developing an electric vehicle discharge simulation framework to evaluate the energy reserves of controllable EV batteries. Using outage zone load criticality and magnitude as prioritised power allocation criteria, this approach minimises outage-induced losses by jointly employing genetic algorithms and refined whale optimisation, ultimately proposing a V2G-centric recovery strategy. Nevertheless, mass centralised dispatch risks accelerating battery degradation cycles, while the model omits implicit cost quantification. Without market-incentive alignment, such technology-driven solutions face severe scalability limitations. Yang et al. (2024b) presents a multi-energy-fusion-based distribution network recovery method, formulating a multi-period restoration model under a flexible, interconnected multi-energy coordination framework. It emphasises coupling constraints among restoration objectives and energy/data/control flows. Utilising data-driven techniques, it replaces convex-hull polyhedral models – prone to excessive conservatism in handling photovoltaic volatility – with a hyperplane polyhedral representation. By embedding uncertainty sets into the restoration model and solving it via a column-and-constraint generation algorithm, this robust framework mitigates conservatism. However, the algorithm's nested main/subproblem optimisation may suffer exponential computation growth as flexible network scales expand. Yang et al. (2024a) advances a recovery method using an enhanced Firefly algorithm, combining global exploration with localised refinement to execute post-fault network islanding. This hybrid accounts for time-varying load attributes and end-user priorities, ensuring critical loads regain power promptly. The refined Firefly algorithm optimises network reconfiguration to maximise restored supply while minimising transmission losses. Yet, its performance hinges on hyperparameters like luminous absorption coefficients and randomised step sizes; slight deviations in large-scale topology adjustments may trigger premature convergence or oscillatory behaviour. Collectively, these studies reveal three persistent challenges:

1 limited real-time processing capability for heterogeneous multi-source data

2 inadequate handling of uncertainties and conflicts in data fusion

3 high computational complexity in solving large-scale stochastic restoration models.

These challenges are often exacerbated in centralised architectures. To overcome these limitations, this paper aims to develop an edge computing-based fast restoration framework that integrates real-time data normalisation, conflict-resilient information

fusion, and a tractable mixed-integer optimisation model, thereby achieving rapid, reliable, and adaptive power recovery for urban medium- and low-voltage networks.

The integration of multimodal data encounters challenges in harmonising disparate feature representations, while semantic disparities between time-series signals and textual inputs hinder cross-modal synergy. Progressive learning frameworks in evolving settings grapple with catastrophic memory loss and must mitigate disturbances induced by shifting data distributions. Few-shot adaptation techniques under weakly labelled conditions exhibit constrained generalisation capacity, frequently suffering from performance deterioration. High-dimensional feature spaces contaminated by noise artefacts and dimensionality inflation impair model adaptability, and latency-sensitive applications further require equilibrium between computational throughput and predictive fidelity. To directly tackle the aforementioned challenges of data latency, fusion conflict, and model complexity, the proposed strategy is built upon three core technical pillars:

1 distributed edge computing architecture for real-time data acquisition and localised processing

2 a two-stage data fusion framework integrating Box-Cox-Z normalisation for non-Gaussian time-series and PCA-enhanced D-S evidence theory for conflict resolution

3 a stochastic optimisation model transformed into a tractable mixed-integer quadratically constrained program via sample average approximation (SAA) and second-order cone relaxation.

The edge computing paradigm overcomes cyber-physical coordination barriers, with decentralised data workflows enabling instantaneous normalisation of heterogeneous multisource inputs. A Box-Cox-enhanced generalised Z-score normalisation technique refines temporal feature capture for non-Gaussian sequences, while PCA-augmented Dempster-Shafer (DS) evidence theory strengthens discordant data assimilation. The multi-criteria restoration formulation is converted into an analytic hierarchy matrix for stochastic approximation treatment, integrated with second-order cone relaxation to establish a mixed-integer quadratically constrained programming architecture, substantially boosting restoration responsiveness and decision stability.

2 Edge computing-based data acquisition and fusion for distribution networks

Edge computing decentralises computational processing and data storage capabilities to peripheral network nodes, enabling minimal-delay responses to satisfy the urgent temporal demands of power system restoration. Immediate processing near generation sources efficiently eliminates signal interference while enhancing primary data integrity, thereby supplying dependable inputs for subsequent operational determinations (Aziz et al., 2022; Hou et al., 2023; Volkova et al., 2024). The decentralised framework prevents network overload resulting from concentrated transmission of extensive monitoring datasets while alleviating communication burdens on core infrastructure. Peripheral nodes autonomously execute regional topology examinations and condition evaluations, significantly compressing the feedback cycle between fault detection and restoration planning. Local integration of diverse data types eliminates conventional centralised

information segregation, establishing comprehensive system-wide awareness. This structural approach improves resilience against individual component failures, guaranteeing preservation of essential functions during critical scenarios. Edge-enabled solutions empower distribution network endpoints with autonomous decision-making capacities, transforming outage recovery from complete reliance on central control directives. The principle of localised data processing aligns with electrical monitoring system security protocols, mitigating potential exposure of confidential data. The tiered model combining distributed intelligence with centralised cloud coordination establishes an adaptable technological platform for forthcoming distribution network modernisation initiatives.

Edge computing architecture is shown in Figure 1.

Figure 1 Edge computing architecture (see online version for colours)

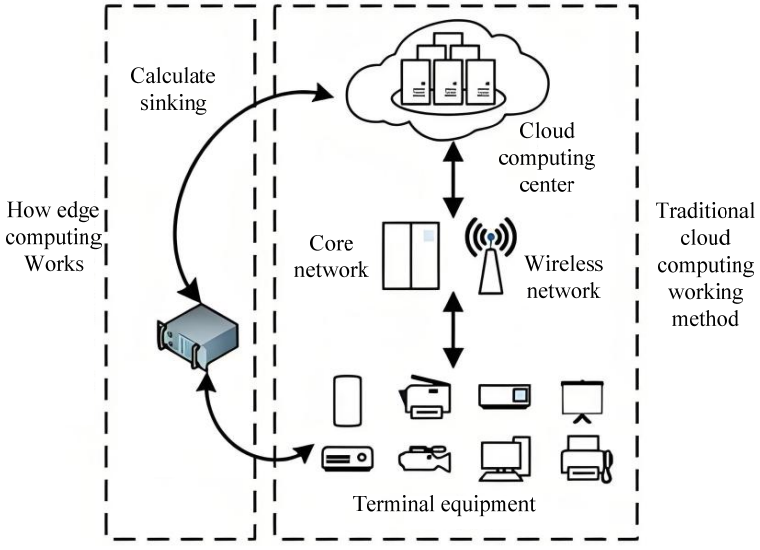

2.1 Multi-source data collection and standardisation

Following the edge computing architecture described above, this section details the multi-source data collection and standardisation process.

During urban power grid restoration for medium and low voltage networks, operational data exhibits substantial variations in structure, units, formats, and volume across different sources (Naik et al., 2023; Jafarpour and Amirioun, 2023). This multi-source heterogeneity introduces three primary technical challenges:

1 temporal misalignment and inconsistent sampling rates among data streams

2 non-Gaussian distributions and skewness in time-series measurements

3 high-dimensional, sparse, and noisy data characteristics that impede direct fusion.

Additionally, the unique features of distribution network data include strong spatiotemporal coupling, real-time volatility due to fluctuating loads and generation, and varying data quality from diverse sensing devices. To enable effective edge-based data

integration and sophisticated information extraction for accelerated power restoration, these inconsistencies must be resolved through comprehensive multi-source data normalisation. Addressing the temporal patterns in distribution system big data, this research introduces an enhanced standardisation approach combining Box Cox transformation with conventional Zscore methodology, creating a generalised power transformation Zscore technique for processing diverse distribution network data sources.

The conventional Zscore standardisation approach presumes that multi-source heterogeneous data factors adhere to a normal distribution. When time-series data exhibit skewness and kurtosis characteristics that violate this assumption, certain factors may receive disproportionately high or low scores during processing. Box Cox transformation, as a generalised power-based adjustment method, effectively addresses cases where continuous response variables deviate from normality. By applying this transformation, it mitigates fluctuations and biases introduced by multi-source time-series data in distribution network operations or data collection, thereby enhancing the precision and dependability of standardised multi-source heterogeneous data processing.

The specific execution steps are as follows:

Step 1 Temporal decomposition is performed on the acquired multi-source urban medium/low-voltage distribution network data. Taking X as standardised transformation input, this X may adopt multi-dimensional data format, matrix representation or vector configuration. With $X = (X_1, X_2, \ldots, X_p)$ configured for matrix representation:

$$X = \begin{bmatrix} x_{11} & x_{12} & \cdots & x_{1p} \\ x_{21} & x_{22} & \cdots & x_{2p} \\ \vdots & \vdots & \ddots & \vdots \\ x_{n1} & x_{n2} & \cdots & x_{np} \end{bmatrix} \tag{1}$$

Step 2 Considering the distinctive attributes of diverse, heterogeneous big data in medium/low voltage distribution systems, BC Z-score normalisation strategies are formulated for various data formats to enable seamless cross-source data conversion.

1 When X appears in vector form, output the transformed result vector $BC\_Z = [X - mean(X)] / \text{std}(X)$.

2 When X appears in vector form, output the transformed result vector BC_Z.

3 For X represented in matrix format, column-wise normalisation applies by utilising sequential mean and standard deviation computations of each column vector, generating the transformed output matrix BC_Z (Panda and Subudhi, 2025).

4 In cases where X adopts a multi-dimensional array structure, computation of mean values and standard deviations occurs across various dimensions of X, enabling subsequent data normalisation procedures that yield the transformed high-dimensional array BC_Z.

Step 3 After undergoing BC Z-score data normalisation processing, $X = (X_1, X_2, \ldots, X_p)$:

$$X^* = \begin{bmatrix} x_{11}^* & x_{12}^* & \cdots & x_{1p}^* \\ x_{21}^* & x_{22}^* & \cdots & x_{2p}^* \\ \vdots & \vdots & \ddots & \vdots \\ x_{n1}^* & x_{n2}^* & \cdots & x_{np}^* \end{bmatrix} \tag{2}$$

Among them:

$$x_{ij}^* = \left(x_{ij} - \overline{x}_j\right) \Big/ \sqrt{s_{ij}} \tag{3}$$

In the formula, $\overline{x}_j$ represents the average value of the solved variable X_j, and $\sqrt{s_{ij}}$ represents the standard deviation of the solved variable X_j.

After completing the BC Z-score data conversion operation, each column of data in $X = (X_1, X_2, \ldots, X_p)$ exhibits the characteristics of $\sqrt{s_{ij}} = 1$ and $\overline{x}_j = 0$.

Step 4 Implement iterative data refinement following the established multi-source processing protocol, cyclically executing the procedures outlined in steps 2 and 3, culminating in the consolidation of all data transformation outcomes.

Step 5 Once all input data sources for the task have undergone dimensional and magnitude normalisation and unification, the processed results are instantly archived to support multi-source data integration, edge computing operations, or long-term data preservation. This concludes the standardisation procedure for heterogeneous data sources.

2.2 Multi-source data fusion model

By utilising edge computing for the integration of diverse data sources in urban medium- and low-voltage distribution networks, only minimal streamlined data processing is required. Consequently, the efficacy and significance of data merging play a pivotal role, as they fundamentally influence the outcomes of distribution network status assessment (Tao et al., 2025; Xie et al., 2024). The core contribution of this section lies in the proposal of a conflict-optimised, PCA-enhanced DS fusion framework, which addresses two fundamental limitations of conventional DS theory in distribution network applications:

1 the inability to handle high-dimensional conflicting evidence effectively

2 the lack of adaptability to dynamically evolving data streams in edge environments.

Our fusion model innovatively integrates principal component analysis (PCA) as a pre-processing dimensionality reduction and conflict isolation stage, followed by a customised DS combination rule that incorporates adaptive reliability weighting derived from real-time data credibility assessment. This two-stage learning structure – dimensionality reduction and conflict decomposition followed by evidence synthesis – enables robust fusion under high uncertainty and noise, which is a marked advancement over static, full-dimensional DS approaches. Following the normalisation of multi-source data, a fusion model is constructed based on the conflict-optimised DS inference framework, which consolidates heterogeneous data from various origins through fusion

techniques, ultimately yielding superior precision compared to edge computing reliant on singular data sources.

The proposed PCA-enhanced DS fusion algorithm is characterised by three key innovations:

1 Conflict-aware dimensionality reduction: PCA is applied prior to DS fusion to extract orthogonal principal components from high-dimensional evidence, effectively isolating conflicting information into lower-dimensional subspaces and mitigating the 'conflict explosion' problem in conventional DS theory.

2 Adaptive evidence weighting: A real-time credibility assessment mechanism dynamically adjusts the reliability weights of evidence sources based on data quality and consistency, enhancing fusion robustness under noisy or uncertain edge environments.

3 Computational efficiency: By reducing dimensionality before fusion, the algorithm significantly lowers computational overhead, making it suitable for latency-sensitive restoration applications.

These contributions collectively address the limitations of existing DS methods in handling high-dimensional, conflicting, and dynamically evolving data streams in distribution networks.

The D-S evidence theory is a widely used framework for data fusion under uncertainty. It extends Bayesian probability theory by eliminating the need for prior probabilities and effectively representing ambiguous or unknown states. Its versatility has led to broad adoption in multi-domain data integration applications. Nevertheless, when implementing DS inference on conflicting subsets, the normalisation procedure within its combination rules frequently produces outcomes inconsistent with the logical merging of disparate data origins. To address this, PCA is employed to refine the DS method for integrating contradictory data sources. PCA facilitates the identification of m (where $m < n$) novel components, enabling these derived elements to encapsulate essential characteristics of discordant information. This approach prioritises the isolation and utilisation of principal conflict components rather than indiscriminately assigning them to undefined categories. Components excluded from fusion are filtered via a predefined credibility function governing their usability.

$$\tilde{k} = \sum_{k=1}^{n} e_i BV_{i,k} \tag{4}$$

In the formula, $\tilde{k}$ serves as an indicator for measuring inter-component conflict intensity, e_i denotes various conflicting factors within the conflict dataset, while $BV_{i,k}$ aligns with particular dimensional attributes present in the conflict information.

Considering the common traits of urban low-voltage power grid big data – including variety in data types, multiplicity of sources, and indeterminate conditions – information gathered from different monitoring endpoints and data origins can be distilled and condensed into characteristic attribute subsets. This enables the integration of heterogeneous multi-source data at the feature tier within power distribution systems (Mwifunyi et al., 2023). The precise implementation methodology proceeds as follows:

Step 1 Initialise the basic probability for the subset of multi-source feature attributes, and set U as the architecture identifier for the multi-source data fusion model of the distribution network. In this case, the function m: $2^U \rightarrow [0, 1]$ needs to meet the following two conditions:

$$\begin{cases} m(A) = 0 \\ \sum\limits_{A \subset U} m(A) = 1 \end{cases} \tag{5}$$

In the formula, $m(A) = 0$ constitutes the initial value for the multi-source data fusion collection A, with $m(A)$'s numerical value indicating the confidence degree attributed to this particular collection.

Step 2 Define credibility evaluation criteria to compute precise belief measure values for integrated datasets resulting from the cross-categorical merging and combination of diverse data types.

$$\begin{cases} Bel : 2^U \rightarrow [0, 1] \\ Bel(A) = \sum\limits_{B \subset A} m(B), \forall A \subset U \end{cases} \tag{6}$$

In the formula, $Bel(A)$ signifies the cumulative probability distribution across all subsets contained within the multi-source data fusion collection A. This analytical structure assigns probabilistic weights that numerically express reliability metrics based on synthesised feature properties linked to each subset. Such quantification demonstrates the distribution network's heterogeneous feature components residing in this ensemble possess the essential capacity to execute core data unification functions.

Step 3 Establish probabilistic assessment criteria for heterogeneous data integration, serving to quantify confidence metrics associated with merged sets of ambiguous feature parameters. The usable proportion of indeterminate feature elements is governed by derived component reliability coefficient $\tilde{k}$, with the exact computational formulation expressed below:

$$\begin{cases} pl(A) = 1 - Bel(\overline{A}) = \sum\limits_{B \subset U} m(B) - \sum\limits_{B \subset \overline{A}} m(B) \\ \tilde{k}_{A \cap B} = \sum\limits_{k=1}^{n} e_i BV_{i,k} \end{cases} \tag{7}$$

In the formula, $pl(A)$ denotes the collection of variables containing uncertain feature attributes with potential fusion capability within multi-source data fusion set A, whereas $\tilde{k}_{A \cap B}$ signifies the reliability metric associated with conflicting components in set A during the integration process of these uncertain feature attributes.

Step 4 Calculate the trust range corresponding to data fusion. According to the correlation between the trust function and likelihood function: $pl(A) \geq Bel(A)$, $A \subset U$, the uncertainty of A can be expressed as:

$$\mu(A) = pl(A) - Bel(A) \tag{8}$$

In the formula, $pl(A) - Bel(A)$, as a trust category, is reflected in the process of multi-source data fusion, which is based on the uncertainty characteristic attributes that are allowed to change in the actual application of the distribution network.

Step 5 Integration and processing of multi-source heterogeneous data feature attributes. When $\forall A \subset U$, on the multi-source data fusion model architecture U of the distribution network, the Dempster fusion rule followed for a finite number of *mass*-functions m_1, m_2, …, m_n is as follows:

$$\left(m_1 \oplus m_2 \oplus \cdots \oplus m_n\right)(A) = \frac{1}{K} \sum_{A_1 \cap A_2 \cap \cdots \cap A_n = A} m_1\left(A_1\right) \cdot m_2\left(A_2\right) \cdots m_n\left(A_n\right) \tag{9}$$

In the formula, K represents the number of iterations.

In compliance with the integration standards, feature-level data combination is accomplished through the application of characteristic parameter indicators derived from multiple data origins.

3 Fast power restoration model for distribution networks

3.1 Objective function and constraints

The edge computing framework has established fundamental technical support for power grid data collection and integration, enabling immediate analysis adjacent to information generation points. This decentralised computational approach simultaneously addresses normalisation challenges of varied multi-source data while delivering premium quality inputs for subsequent data consolidation algorithms.

The primary purpose of goal configuration is to attain the optimal cumulative retrieved capacity weighting, establish peak equilibrium in zones experiencing no electricity deprivation, and minimise dissipation of energy throughout the electrical network.

$$f_1 = \sum_{i \in \Omega_n} \omega_i \lambda_i P_i^{Load} \tag{10}$$

$$f_2 = \frac{1}{n_{NL}} \sum_{ij \in n_{NL}^h} \frac{I_{ij}}{I_{ij,\max}} \tag{11}$$

$$f_3 = \sum_{ij \in \Omega_b} r_{ij} I_{ij}^2 + \sum_{n \in \Omega_{SOP}} P_{SOP,n}^{loss} \tag{12}$$

In the above formula, ω_i represents the critical weight coefficient of the load carried by position λ_i, λ_i represents the recovery efficiency coefficient, P_i^{Load} represents the active power value of the load on node i, Ω_n represents the node with power interruption, n_{NL} represents the total number of power supply areas that have not experienced power

outage, and n_{NL}^{b} represents the feeder line within the power outage area; $I_{ij,\max}$ represents the maximum current allowed by the system, Ω_b represents the branch lines within the system, and $P_{SOP,n}^{loss}$ represents the power loss of the SOP device.

Using judgment matrix methods to achieve the transformation from multiple objectives to a single objective:

$$f = \min\left(-\mu_1 f_1 + \mu_2 f_2 + \mu_3 f_3\right) \tag{13}$$

Construct a matrix in the following form using the judgment matrix method:

$$J = \begin{bmatrix} 1 & 5 & 3 \\ 1/5 & 1 & 3 \\ 1/7 & 1/3 & 1 \end{bmatrix} \tag{14}$$

After processing, the weight vectors of each target are obtained:

$$\begin{bmatrix} \mu_1 & \mu_2 & \mu_3 \end{bmatrix} = \begin{bmatrix} 0.7235 & 0.1932 & 0.0833 \end{bmatrix} \tag{15}$$

The constraints of the objective function are as follows:

1 Trend constraints

$$\begin{cases} P_i = P_i^{DG} + P_{SOP,i} - \lambda_i P_i^{Load} \\ Q_i = Q_i^{DG} + Q_{SOP,i} - \lambda_i Q_i^{Load} \\ \sum\limits_{ik\in\Omega_b} P_{ik} = \sum\limits_{ji\in\Omega_b} \left(P_{ji} - R_{ji} I_{ji}^2\right) - P_i \\ \sum\limits_{ik\in\Omega_b} Q_{ik} = \sum\limits_{ji\in\Omega_b} \left(Q_{ji} - R_{ji} I_{ji}^2\right) - Q_i \\ U_j^2 = U_i^2 - 2\left(R_{ij} P_{ij} + X_{ij} Q_{ij}\right) + \left(R_{ij}^2 + X_{ij}^2\right) I_{ij}^2 \\ I_{ij}^2 = \dfrac{R_{ij}^2 + Q_{ij}^2}{U_i^2} \end{cases} \tag{16}$$

In the formula, U^i represents the voltage value at position i, R_{ij} and X_{ij} are the impedance parameters corresponding to branches i and j, P^{ij} and Q^{ij} are the active and reactive power values at position i, and Q_i^{Load} represents the reactive power value of the load at position i.

2 SOP operation constraints

The expressions for SOP active power constraint and capacity constraint are shown in formulas (17) and (18), respectively:

$$\begin{cases} \sum\limits_{n\in1,2,3} P_{SOP,n} + \sum\limits_{n\in1,2,3} P_{SOP,n}^{loss} = 0 \\ P_{SOP,n}^{loss} = A_{SOP,n} \sqrt{P_{SOP,n}^2 + Q_{SOP,n}^2} \end{cases} \tag{17}$$

$$\sqrt{P_{SOP,n}^2 + Q_{SOP,n}^2} \le S_{SOP,n} \tag{18}$$

In the above formula, n represents the number of VSCs, $P_{SOP,n}$ and $Q_{SOP,n}$ represent the active and reactive power injected by VSCs, $P_{SOP,n}^{loss}$ represents the losses generated by VSCs, $A_{SOP,n}$ represents the loss coefficient of VSCs, and $S_{SOP,n}$ represents the capacity of SOP.

3 Voltage over limit chance constraint

$$\begin{cases} p_r\left\{\left|U_i'\right| \geq U_{\min,i}^2\right\} \geq p_{U_{\min,i}^2} \\ p_r\left\{\left|U_i'\right| \leq U_{\max,i}^2\right\} \geq p_{U_{\max,i}^2} \end{cases} \tag{19}$$

In the formula, $p_r\{\}$ is used to refer to the probability function of event occurrence, $U_{\max,i}$ and $U_{\min,i}$ represent the upper and lower limits of voltage, and p is used to indicate the degree of confidence. Formula (19) indicates that the probability of the voltage amplitude being within the specified range needs to exceed the established confidence level.

3.2 Deterministic model transformation

SAA is a widely adopted Monte Carlo simulation-based technique for solving stochastic optimisation problems by approximating the expected objective function and probabilistic constraints through a finite set of random samples. In the context of power system restoration under uncertainty, SAA transforms the original stochastic program – which involves complex, high-dimensional probability distributions – into a deterministic counterpart that is computationally tractable. The core principle relies on the law of large numbers, ensuring that as the sample size increases, the sample average converges almost surely to the true expected value. This allows the replacement of intractable probabilistic constraints with deterministic equivalents based on empirical distributions, thereby enabling the application of conventional mixed-integer programming (MIP) solvers.

Employing the SAA technique, the stochastic optimisation challenge is converted into a deterministic formulation. The SAA approach defines the voltage limit violation constraint as follows:

$$\begin{cases} N_S^{-1}\sum_{j=1}^{N_S} D_{\min,u}\left(U_{\min,i}^2 - \left|U_i'\right| \geq 0\right) \leq \gamma_{\min,u} \\ D_{\min,u}\left[F(x,\xi^j)\right] = \begin{cases} 1, \text{if } U_{\min,i}^2 \geq \left|U_i'\right| \\ 0, \text{if } U_{\min,i}^2 < \left|U_i'\right| \end{cases} \\ N_S^{-1}\sum_{j=1}^{N_S} D_{\max,u}\left(\left|U_i'\right| - U_{\max,i}^2 \geq 0\right) \leq \gamma_{\max,u} \\ D_{\max,u}\left[F\left(x,\xi^j\right)\right] = \begin{cases} 1, \text{if } \left|U_i'\right| \geq U_{\max,i}^2 \\ 0, \text{if } \left|U_i'\right| < U_{\max,i}^2 \end{cases} \end{cases} \tag{20}$$

In the formula, N_S represents the number of samples taken, ξ^j represents the sample taken in a certain cycle, γ represents the confidence level value, and $D_{\max,u}[F(x, \xi^j)]$ represents the indicative function. Due to the non-convex characteristics of indicator functions, the initial formula remains incapable of being immediately resolved and classified under

binary 0-1 constraint conditions. Consequently, the SAA challenge is converted into a MIP formulation subject to the subsequent limitations:

$$\begin{cases} U_{\min,i}^2 - \left|U_i'\right| \le Mz_{j,\min},\ j = 1, ..., N_S \\ \left|U_i'\right| - U_{\max,i}^2 \le Mz_{j,\max},\ j = 1, ..., N_S \end{cases} \tag{21}$$

$$\begin{cases} \sum_{j=1}^{N_S} z_{j,\min} \le \gamma_{\min,u} N_S \\ \sum_{j=1}^{N_S} z_{j,\max} \le \gamma_{\max,u} N_S \\ z_{j,\min}, z_{j,\max} \in \{0, 1\} \end{cases} \tag{22}$$

In the above formula, M takes a positive value and z is a binary 0-1 variable introduced to replace the indicator function. In formula (21), if $z_j = 0$, it means that in the j^{th} sampling scenario, there was no voltage exceeding the limit condition; If $z_j = 1$, it indicates that no voltage limitation has been applied to the j^{th} sampling scenario. Equation (16) imposes restrictions on instances where voltage measurements fall outside the permissible range, both below the lower threshold and above the upper limit. Following this methodology, the probabilistic constraint is converted into a definitive linear constraint formulation.

To meet the standard constraint form required by the second-order cone, I_{ij}^2 and U_i^2 are replaced with I_{ij}' and U_i' respectively, and the SOP constraint is transformed into a rotating cone form constraint. Finally, the following results are obtained:

$$\begin{cases} P_{SOP,n}^2 + Q_{SOP,n}^2 \le 2\left(\dfrac{P_{SOP,n}^{loss}}{\sqrt{2} A_{SOP,n}}\right)^2 \\ P_{SOP,n}^2 + Q_{SOP,n}^2 \le 2\left(\dfrac{S_{SOP,n}}{\sqrt{2}}\right)^2 \end{cases} \tag{23}$$

Next, convert formula (16) into the relaxed form of a second-order cone:

$$\left\| \begin{bmatrix} 2P_{ij} & 2Q_{ij} & I_{ij}' - U_i' \end{bmatrix} \right\| \le I_{ij}' + U_i' \tag{24}$$

Building upon these theoretical foundations, the accelerated recovery framework for metropolitan medium-low voltage power distribution systems incorporating probabilistic constraints can be reformulated as a definite mixed-integer quadratic constrained optimisation challenge, amenable to direct resolution via mathematical programming solvers.

4 Test experiment

4.1 Experimental environment and data

To validate the proposed restoration model, experiments were conducted on a realistic urban distribution network with the following configuration.

The experimental investigation was performed on five linked feeders within an urban 10 kV medium-low voltage network. The study incorporated two dispatchable distributed generation systems along these circuits, both possessing 50 kW nominal generation capacities, alongside an energy storage facility rated at 100 kWh. Designated residential zones further included flexible demand-side loads featuring regulation capabilities, demonstrating maximum power consumption of 80 kW. Refer to Figure 2 for the schematic representation.

Figure 2 Simplified schematic diagram of system wiring

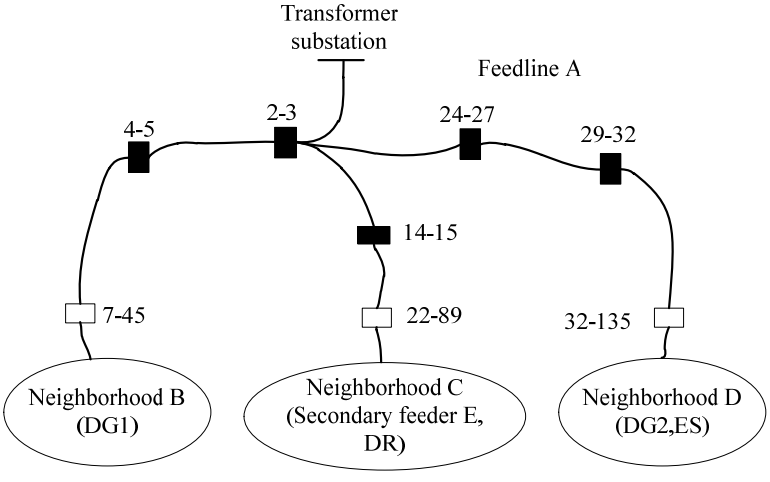

The first level feeder support situation is shown in Table 1.

Table 1 Supporting factors included in the primary feeder line

Primary feeder	*Supporting factors included*	*Support factor node/contact switch*
Feeder B	DG1	81
Feeder C	Feeder E (secondary feeder)	94–146
	DR load	89
Feeder D	ES	101
	DG2	119

Employing maximum historical demand figures as baseline criteria, establish a normalised 100% reference scale. Various demand intensity conditions are replicated through uniform application of an X% multiplier (designated as the demand variation coefficient with $X < 100$) to all nodal consumption values. During area A's outage condition, primary circuits B, C and D maintaining service exhibited demand variation coefficients of 93%, 82% and 88% respectively. Performance metrics for these three operational primary circuits are specified in Table 2, excluding any influence from distributed generation systems interconnected with the network.

Table 3 displays the operational characteristics of distributed generation units, storage systems, and demand-side responsive loads integrated into the network. During active operation, the storage system delivers consistent power output at its nominal 120 kW

capacity, while the demand-responsive loads typically maintain consumption levels above 150 kW during standard functioning.

Table 2 Operation of primary feeders B, C, and D

Feeder name	*B*	*C*	*D*
Load factor (X%)	93%	82%	88%
Substation active power output/MW	3.7935	1.5973	4.9196
Total active load of the line/MW	3.7539	1.5848	4.6841
Total active load of the line/Mvar	1.0949	0.4622	1.3662

Table 3 DG, ES, DR load parameters

Name	*Rated power/kW*	*Maximum power/kW*	*Maximum adjustable power/kW*
DG1	150	230	80
DG2	120	170	50
ES	120	-	120
DR load	-	-	150

4.2 Test plan and indicators

Compare the method proposed in this paper with the methods in Yang et al. (2024a, 2024b) based on indicators such as power restoration time, power restoration success rate, and load balancing degree.

- Duration of electrical service restoration: This metric quantifies the interval between distribution system failure initiation and full re-establishment of electricity delivery to impacted customers. As a direct manifestation of utility companies' rapid incident resolution proficiency and crisis management effectiveness, it serves as a crucial operational benchmark for assessing metropolitan power grid maintenance standards and customer service performance. Reduced restoration intervals correlate with enhanced incident mitigation efficiency and diminished consumer disruption impacts, holding particular relevance for safeguarding uninterrupted energy provision to critical facilities while simultaneously functioning as a principal evaluation criterion for assessing intelligent grid autonomous recovery capabilities.
- Fault recovery achievement percentage: This fundamental metric assesses holistic effectiveness in addressing electrical network disruptions, quantifying the proportion of customers regaining service within mandated timeframes relative to total impacted consumers. Beyond measuring automated grid equipment functionality, this parameter demonstrates operational management framework robustness and contingency protocol efficacy. Elevated restoration percentages signal distribution systems possessing resilient autonomous recovery mechanisms and optimised topological configurations, effectively mitigating service interruption consequences while guaranteeing uninterrupted electricity delivery – a vital benchmark reflecting contemporary smart grid infrastructure implementation success.
- Current distribution equilibrium metric: Serving as a crucial parameter for assessing post-restoration grid operational economics and safety, this measurement

numerically expresses load allocation uniformity through statistical evaluation of individual feeder circuit utilisation variances. The metric directly reveals network reconfiguration strategy appropriateness and electrical service recovery scheme optimisation effectiveness. Optimal current distribution prevents regional conductor overloading while simultaneously enhancing asset employment efficiency, prolonging infrastructure lifespan, decreasing transmission dissipation, and boosting comprehensive grid performance efficiency.

4.3 Analysis of test results

4.3.1 Power restoration time

The duration required for electricity reinstatement in urban low-voltage grids critically influences consumer power consumption quality and uninterrupted socioeconomic operations. Rapid recovery capability serves not merely as a factor in grid stability maintenance, but functions as a decisive benchmark assessing contemporary distribution systems' intelligent advancement. Focused experimentation enables precise assessment of fault identification, section isolation and load transfer responsiveness, while detecting both technological deficiencies and administrative vulnerabilities. Experimental metrics offer measurable evidence for enhancing emergency resource distribution and refining autonomous operation tactics, facilitating an operational paradigm transition from reactive troubleshooting to anticipatory protection. Comparative electricity restoration durations across three tested approaches are presented in Table 4.

Table 4 Results of power supply recovery time

Number of tests	*Power restoration time/min*		
	Proposed method	*Yang et al. (2024b) method*	*Yang et al. (2024a) method*
1	3.45	25.67	38.92
2	4.12	28.34	42.15
3	2.98	23.78	36.54
4	3.76	26.89	40.23
5	4.53	29.56	44.78
6	2.89	22.45	35.10
7	3.91	27.21	41.67
8	4.27	30.89	45.90
9	3.33	24.50	37.89
10	4.00	26.12	39.56

As shown in Table 4, the proposed method consistently achieved restoration times under 5 minutes, with a maximum of 4.53 minutes and a minimum of 2.89 minutes, resulting in a narrow performance deviation of only 1.64 minutes. Comparatively, the technique from Yang et al. (2024b) exhibited prolonged resolutions exceeding 20 minutes with an 8.44-minute variance, while Yang et al. (2024a) consistently required over 35 minutes with fluctuations surpassing 10 minutes. Our solution achieves dual breakthroughs: dramatically compressing fault-resolution durations while delivering unmatched temporal consistency – conclusive evidence of revolutionary advancements in fault-precision

targeting and automated remediation speed. This order-of-magnitude superiority highlights conventional methods' technological obsolescence in fault segregation and grid reconfiguration, whereas our intelligent protocol satisfies contemporary distribution networks' exacting demands for rapid service recovery.

The significantly shorter and more stable restoration time achieved by the proposed method can be attributed to the synergistic effect of its core technical components. Firstly, the edge computing architecture enables decentralised data processing, which eliminates the communication latency inherent in centralised methods like those in Yang et al. (2024a, 2024b). This allows for near-instantaneous fault detection and localisation. Secondly, the efficient Box-Cox-Z normalisation and PCA-enhanced DS fusion rapidly generate a coherent and accurate system state estimation from heterogeneous data, reducing the time spent on data reconciliation. Finally, the tractable MICQP model, transformed via SAA and second-order cone relaxation, can be solved much faster than the complex stochastic or heuristic models used in the comparative methods. This integrated pipeline from data to decision minimises each phase's delay, resulting in the observed sub-5-minute recovery capability.

4.3.2 Success rate of power restoration

Power restoration success percentage serves as a critical metric for assessing urban grid performance in fault response effectiveness and energy delivery consistency. Evaluating this parameter enables impartial judgment of mechanical precision in automated devices, procedural compliance among technical staff, and strategic soundness in power grid reconfiguration approaches. Persistent underperformance in this metric risks triggering cascading system failures or extensive service disruptions. Systematic tracking of restoration success facilitates early detection of latent technical deficiencies, refinement of protection coordination mechanisms, and improvement of cross-departmental emergency response synergy. These measurements constitute fundamental evidence when validating smart terminal deployment completeness and feeder automation sophistication, offering targeted guidance for distribution network modernisation while guaranteeing sub-second autonomous power recovery even during intricate fault conditions. Comparative restoration success rates across three methodologies are illustrated in Figure 3.

The graphical representation in Figure 3 clearly illustrates the superior performance characteristics of our novel approach regarding power restoration effectiveness. Across 10 experimental trials, our technique consistently achieved a remarkable 95% success rate with zero performance variations, showcasing exceptional operational consistency and dependability. These results confirm that the automated systems function with precision, maintenance teams follow strict protocols, and the grid reconfiguration methodology demonstrates optimal efficiency – collectively preventing recurrent faults and minimising service interruption durations. Comparative analysis reveals that the technique from Yang et al. (2024b) exhibits substantial performance volatility, ranging from a minimum 60% to peak 78% success rate, suggesting potential inconsistencies in device accuracy, personnel procedures, or network restructuring logic. While Yang et al. (2024a) show more consistent outcomes, its plateau between 70%–75% success rate suggests opportunities for enhanced fault resolution speed and electrical service continuity.

The consistently high (95%) success rate stems primarily from the robustness of the data fusion and optimisation model against uncertainty and conflict. The key mechanism is the conflict-optimised, PCA-enhanced DS fusion framework. By isolating and managing conflicting evidence through PCA and adaptive weighting, the method avoids the generation of misleading system states that could trigger incorrect switching sequences – a common cause of restoration failure in conventional methods. Furthermore, the SAA-handled chance constraints in the optimisation model ensure that the restoration plan is feasible under a wide range of uncertain scenarios (e.g., fluctuating DG output or load), thereby increasing the probability of successful execution. In contrast, the methods in Yang et al. (2024a, 2024b) are more susceptible to data conflict and model conservatism, leading to higher failure rates and greater performance volatility.

Figure 3 Results of power supply recovery success rate (see online version for colours)

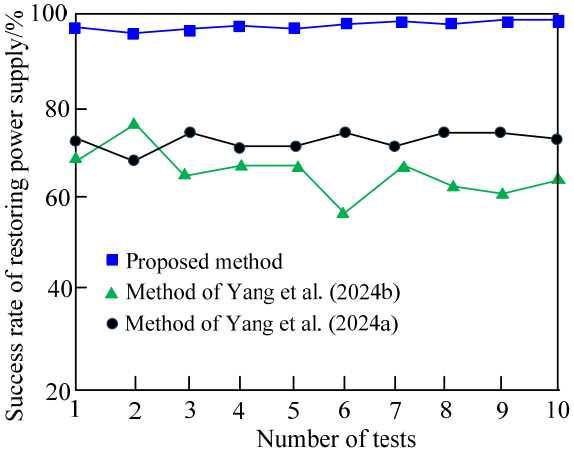

4.3.3 Load balancing degree

Load equilibrium assessment serves as a crucial benchmark for judging operational excellence in electrical networks post-restoration. Excessive load concentration risks triggering subsequent malfunctions including equipment overburden and voltage instability, compromising the genuine effectiveness of swift power recovery. Precise numerical analysis enables comprehensive understanding of distribution line and transformer capacity limits while validating the soundness of load redistribution approaches. This parameter fundamentally influences the endurance of restoration schemes, offering vital informational foundations for real-time adjustments in distributed generation output and grid architecture refinements, thereby guaranteeing that post-fault power networks exhibit rapid responsiveness and prolonged steady-state operation. Comparative equilibrium performance metrics across the three methodologies are presented in Table 5.

Table 5 reveals that the load balancing metric of our approach consistently stays within the narrow band of 0.82 to 0.91, exhibiting a minimal variation span of merely 0.09, which underscores its exceptional steadiness. On the other hand, the balancing indices of the techniques from Yang et al. (2024a, 2024b) oscillate between 1.25–1.42

and 1.39–1.55, respectively, showing larger fluctuations of 0.17 and 0.16, while their readings persistently exceed those of our proposed methodology. At every one of the ten measured intervals, our method's equilibrium value remains under 1.0, confirming that its load allocation perpetually achieves an optimal uniform distribution, whereas competing methods sustain disparities exceeding 1.25-fold. This combination of low numerical values and superior consistency successfully mitigates the potential for equipment overloading and ensures dependable support for power system recovery quality. Notably, even during peak demand phases at 40 and 90 minutes, our solution sustains outstanding performance with values below 0.90, showcasing a clear technical edge over the rival methods' elevated load imbalances of 1.42 and 1.40.

Table 5 Load balancing degree

Time/min	*Load balancing degree*		
	Proposed method	*Yang et al. (2024b) method*	*Yang et al. (2024a) method*
10	0.85	1.32	1.45
20	0.88	1.28	1.50
30	0.82	1.35	1.40
40	0.90	1.42	1.55
50	0.87	1.30	1.48
60	0.84	1.38	1.42
70	0.89	1.25	1.52
80	0.86	1.33	1.47
90	0.91	1.40	1.39
100	0.83	1.37	1.51

The superior and stable load balancing performance (0.82–0.91) is a direct consequence of the multi-objective optimisation formulation and the accurate system modelling within the MICQP framework. The underlying mechanism involves two aspects:

1 The objective function explicitly includes load balance as a goal [equation (12)], and the analytic hierarchy process effectively coordinates it with other objectives like restoration capacity.

2 The use of second-order cone relaxation accurately models power flow constraints, allowing the optimiser to find a solution that not only restores power but also redistributes loads in a manner that minimises line currents and prevents overloads.

The competing methods either lack an explicit balance objective or rely on approximations that compromise solution quality, resulting in higher and more volatile imbalance indices, which indicate suboptimal network reconfiguration and higher operational risk.

5 Conclusions

Ensuring swift electricity restoration in urban medium- and low-voltage power distribution systems holds critical importance for maintaining urban grid stability,

enhancing living standards, and driving socioeconomic growth. Given the existing challenges where cyber-physical system data coordination struggles with the conflict between dynamically coupled heterogeneous multi-spatiotemporal-scale data and real-time processing demands – resulting in prolonged outage recovery durations – edge computing-based research offers a breakthrough solution. This paper proposed a comprehensive fast restoration method based on a distributed edge computing architecture. Its core advantages lie in three key aspects:

1 the significant reduction in data latency and processing overhead through localised edge intelligence

2 the robust fusion of heterogeneous multi-source data under uncertainty via a PCA-enhanced DS evidence theory framework

3 the formulation of a tractable mixed-integer quadratically constrained programming model for efficient and reliable recovery decision-making.

The key outcomes, validated through experiments, include achieving an average restoration time of under 5 minutes, a success rate exceeding 95%, and a superior load balancing degree between 0.82–0.91. These results demonstrate that the proposed method provides a robust, high-performance solution for urban grid recovery, effectively overcoming the limitations of centralised approaches and significantly elevating power supply reliability.

Declarations

All authors declare that they have no conflicts of interest.

References

Aziz, T., Waseem, M. and Liu, S.L.Z. (2022) 'Two-stage MILP model for optimal skeleton-network reconfiguration of power system for grid-resilience enhancement', *Journal of Energy Engineering*, Vol. 148, No. 1, pp.4021–4031.

Hou, S., Chen, J. and Chen, G. (2023) 'Distributed control strategy for voltage and frequency restoration and accurate reactive power-sharing for islanded microgrid', *Energy Reports*, Vol. 9, No. 6, pp.742–751.

Hu, S., Liao, K., Yang, J. et al. (2023) 'Power supply restoration strategy of urban power grid based on V2G technology', *Electric Power Automation Equipment*, Vol. 43, No. 6, pp.53–61.

Jafarpour, S. and Amirioun, M.H. (2023) 'A resilience-motivated restoration scheme for integrated electricity and natural gas distribution systems using adaptable microgrid formation', *IET Generation, Transmission & Distribution*, Vol. 17, No. 23, pp.5223–5239.

Kayal, P. and Basumatary, R.G. (2023) 'Fostering restoration and power delivery efficiency by distributed generators and line switches in electricity distribution network', *Energy Sources, Part A. Recovery, Utilization, and Environmental Effects*, Vol. 45, No. 2, pp.5864–5884.

Kottmann, F., Kyriakidis, M., Sansavini, G. et al. (2023) 'A human operator model for simulation-based resilience assessment of power grid restoration operations', *Reliability Engineering & System Safety*, Vol. 238, No. 18, pp.109450–109469.

Mannan, A.M., Dang, H.P. and Pico, H.N.V. (2024) 'FIDVR capability of hybrid grid-forming PV power plants during feeder restoration', *IEEE Transactions on Energy Conversion*, Vol. 39, No. 3, pp.1613–1629.

Mwifunyi, R.J., Mnyanghwalo, D.C. and Kawambwa, S.J. (2023) 'Enhancing service restoration in tanzanian power grid using internet of things sensors and renewable energy sources', *Tanzania Journal of Science*, Vol. 49, No. 3, pp.4314–4325.

Naik, P.L., Rambabu, C., Rasululla, S.K. et al. (2023) 'ANFIS control based improve PCC voltage quality of an isolated photovoltaic-wind and hybrid energy restoration micro grid system', *Microsystem Technologies*, Vol. 29, No. 4, pp.563–572.

Panda, S.K. and Subudhi, B. (2025) 'A distributed adaptive super-twisting sliding mode controller for voltage and frequency restoration in islanded microgrid', *IEEE Journal of Emerging and Selected Topics in Power Electronics*, Vol. 13, No. 1, pp.1010–1017.

Tao, W., Feng, L., Peng, K. et al. (2025) 'Power restoration method for distribution network based on optimal configuration of photovoltaic and energy storage in extreme disaster scenarios', *Automation of Electric Power Systems*, Vol. 49, No. 7, pp.189–197.

Volkova, A., Ghasemi, A. and Meer, H.D. (2024) 'Towards forming optimal communication network for effective power system restoration', *IEEE Transactions on Network and Service Managementt*, Vol. 21, No. 5, pp.5250–5259.

Xie, Y., Zhang, D., Yang, Q. et al. (2024) 'A dynamic power supply restoration method for resilient urban power grids considering repair uncertainty and V2G under typhoon disaster', *Power System and Clean Energy*, Vol. 40, No. 6, pp.107–114.

Yang, C., Cheng, T., Li, S. et al. (2023) 'A novel partitioning method for the power grid restoration considering the support of multiple LCC-HVDC systems', *Energy Reports*, Vol. 9, No. 2, pp.1104–1112.

Yang, Y., Liu, Q., Wu, Y. et al. (2024a) 'Fault recovery strategy of distribution network based on improved firefly algorithm', *Modern Electric Power*, Vol. 41, No. 2, pp.287–294.

Yang, Z., Yang, F., Lei, Y. et al. (2024b) 'Data-driven robust service restoration method for flexible interconnected distribution networks based on multi-flow fusion', *High Voltage Engineering*, Vol. 50, No. 8, pp.3508–3524.

Yurov, A. (2022) 'Device for the automatic detection of fault locations during high-voltage insulation testing of power cable lines of electric power systems', *Power Technology and Engineering*, Vol. 56, No. 5, pp.438–440.

Zhang, Z. (2022) 'Limited risk power restoration method for distribution system with user-side microgrid cluster based on cloud-side collaboration', *SSRN Electronic Journal*, DOI: 10.2139/ssrn.4112140.